SARS-CoV-2 B.1.1.7 escape from mRNA vaccine-elicited neutralizing antibodies

Dami A. Collier[1,2,3]*, Anna De Marco[4]* , Isabella A.T.M. Ferreira*[1,2] Bo Meng[1,2]*, Rawlings Datir *[1,2,3], Alexandra C. Walls[5], Steven A. Kemp S[1,2,3], Jessica Bassi[4], Dora Pinto[4], Chiara Silacci Fregni[4], Siro Bianchi[4], M. Alejandra Tortorici[5], John Bowen[5], Katja Culap[4], Stefano Jaconi[4], Elisabetta Cameroni[4], Gyorgy Snell[6], Matteo S. Pizzuto[4], Alessandra Franzetti Pellanda[7], Christian Garzoni[7], Agostino Riva[8], The CITIID-NIHR BioResource COVID-19 Collaboration[9], Anne Elmer[10], Nathalie Kingston[10], Barbara Graves [10], Laura E McCoy[3], Kenneth GC Smith [1,2], John R. Bradley [2,10], James Thaventhiran J[2], Lourdes Ceron-Gutierrez L[11], Gabriela Barcenas-Morales [11,12], Herbert W. Virgin[6], Antonio Lanzavecchia[4], Luca Piccoli[4], Rainer Doffinger[11], Mark Wills[2] , David Veesler[5], Davide Corti[4]*, Ravindra K. Gupta[1,2, 13]*

*Equal contribution

[1]Cambridge Institute of Therapeutic Immunology & Infectious Disease (CITIID), Cambridge, UK.
[2]Department of Medicine, University of Cambridge, Cambridge, UK.
[3]Division of Infection and Immunity, University College London, London, UK.
[4]Humabs Biomed SA, a subsidiary of Vir Biotechnology, 6500 Bellinzona, Switzerland.
[5]Department of Biochemistry, University of Washington, Seattle, WA 98195, USA
[6]Vir Biotechnology, San Francisco, CA 94158, USA.
[7]Clinic of Internal Medicine and Infectious Diseases, Clinica Luganese Moncucco, 6900 Lugano, Switzerland
[8]Division of Infectious Diseases, ASST Fatebenefratelli Sacco, Luigi Sacco Hospital, University of Milan, 20157 Milan, Italy
[9] The CITIID-NIHR BioResource COVID-19 Collaboration, see appendix 1 for author list
[10] NIHR Cambridge Clinical Research Facility, Cambridge, UK.
[11]Department of Clinical Biochemistry and Immunology, Addenbrookes Hospital, UK
[12] Laboratorio de Inmunologia, S-Cuautitlán, UNAM, Mexico
[13] Africa Health Research Institute, Durban, South Africa

Correspondence: dcorti@vir.bio, rkg20@cam.ac.uk

Key words: SARS-CoV-2; COVID-19; antibody, vaccine, neutralising antibodies; mutation;

Abstract

SARS-CoV-2 transmission is uncontrolled in many parts of the world, compounded in some areas by higher transmission potential of the B1.1.7 variant now seen in 50 countries. It is unclear whether responses to SARS-CoV-2 vaccines based on the prototypic strain will be impacted by mutations found in B.1.1.7. Here we assessed immune responses following vaccination with mRNA-based vaccine BNT162b2. We measured neutralising antibody responses following a single immunization using pseudoviruses expressing the wild-type Spike protein or the 8 mutations found in the B.1.1.7 Spike protein. The vaccine sera exhibited a broad range of neutralizing titres against the wild-type pseudoviruses (<1:4 to 3449) that were reduced against B.1.1.7 variant by 3.85 fold (IQR 2.68-5.28). This reduction was also evident in sera from some convalescent patients. Decreased B.1.1.7 neutralization was also observed with monoclonal antibodies targeting the N-terminal domain (9 out of 10), the Receptor Binding Motif (RBM) (5 outof 29), but not in neutralizing mAbs binding outside the RBM. Introduction of the E484K mutation in a B.1.1.7 background led to a further loss of neutralizing activity by vaccine-elicited antibodies over that conferred by the B.1.1.7 mutations alone. Further work is needed to establish the impact of these observations on protective vaccine efficacy in the context of the evolving B.1.1.7 lineage that will likely acquire E484K.

Introduction

The outbreak of a pneumonia of unknown cause in Wuhan, China in December 2019, culminated in a global pandemic due to a novel viral pathogen, now known to be SARS-COV-2[1]. The unprecedented scientific response to this global challenge has led to the rapid development of vaccines aimed at preventing SARS-COV-2 infection and transmission. Continued viral evolution led to the emergence and selection of SARS-CoV-2 variants with enhanced infectivity/transmissibility[2,3] [4,5] and ability to circumvent drug[6] and immune control[7,8].

SARS-CoV-2 vaccines have recently been licensed that target the Spike (S) protein, either using mRNA or adenovirus vector technology with protection rates over a few months ranging from 62 to 95%[9-11]. The BNT162b2 vaccine encodes the full-length trimerised S protein of SARS CoV-2 and is formulated in lipid nanoparticles to optimise delivery to cells[12]. Other vaccines include the Moderna mRNA-1273 vaccine, which is also a lipid nanoparticle formulated S glycoprotein[13] and the Oxford-AstraZeneca ChAdOx1 nCoV-19 vaccine (AZD1222) which is a replication-deficient chimpanzee adenoviral vector ChAdOx1, containing the S glycoprotein[14]. The duration of immunity conferred by these vaccines is as yet unknown. These vaccines were designed against the Wuhan-1 isolate discovered in 2019. Concerns have been raised as to whether these vaccines will be effective against new SARS-CoV-2 variants, such as B.1.1.7 (N501Y.V1), B.1.351 (N501Y.V2) and P1 (N501Y.V2) that

originated in the UK, South Africa, and Brazil and are now being detected all over the world[15-17].

The phase I/II studies of the Pfizer-BioNTech BNT162b2 vaccine determined the immunogenicity of different dosing regimens. The geometric mean concentration (GMC) of RBD-binding IgG 21 days after the first dose of 30 µg of the BNT162b2 vaccine, which is the dose approved in the UK, was higher than the GMC of a panel of convalescent plasma (1,536 vs 602 U/ml). Nevertheless, the corresponding neutralisation geometric mean titre (GMT) was 3-fold lower than a panel of convalescent plasma (29 vs 94)[12], but substantially increased after boost immunization[18]. In older adults mean GMT was only 12 in a preliminary analysis of 12 participants[19] and increased to 109 after the second dose.

In this study, we assess antibody responses induced three weeks after vaccination with the first dose of BNT162b2 following the rollout in the UK. In addition, by using a panel of human neutralizing monoclonal antibodies (mAbs) we show that the B.1.1.7 variant can escape neutralization mediated by most NTD-specific antibodies tested and by a fraction of RBM-specific antibodies. We also show that the recent appearance of the E484K mutation in B.1.1.7 isolates from the UK, similarly to the B.1.351 and P1 isolates, results in incremental loss of neutralization by BNT162b2 mRNA-elicited antibodies.

Results

Twenty-three participants had received the BNT162b2 mRNA vaccine three weeks prior to blood draw for serum and peripheral blood monocnulear cells (PBMC) collection. Median age was 82 years (IQR 64-85) and 30% were female (**Table 1**). Serum IgG titres to N protein, S and the S RBD were assayed by particle based flow cytometry on a Luminex analyser (**Fig. 1a**). These data showed Spike and RBD antibody titres much higher than in healthy controls, similar to both convalescent plasma units used for therapeutic purposes as well as to serum from recovered individuals. The raised N titres relative to control could be the result of non specific cross reactivity that is increased following vaccination. However, the antibody response was heteorgenorus withalmost 100-fold variation in IgG titres to S and Spike RBD across the vaccinated participants.

Using lentiviral pseudotyping we generated wild type S proteins on the surface of enveloped virions in order to measure neutralisation activity of vaccine-elicited sera. This system has been shown to give results correlating with replication competent authentic virus[20,21]. The vaccine

sera exhibited a range of inhibitory dilutions giving 50% neutralisation (ID50) ≤4 to 3449 (**Fig. 1c-d**). The GMT against wild type (WT) pseudovirus was 24. Eight out of 23 participants exhibited no appreciable neutralisation against the WT pseudotyped virus. There was reasonable correlation between full length S IgG titres and serum neutralisation titres (**Extended Data Fig. 1a**). A broad range of T cell responses was measured by IFN gamma FLUOROSPOT against SARS-CoV-2 peptides in vaccinees. These cell responses did not correlate with IgG S antibody titres, but there was some correlation with serum neutralisation against WT virus (**Extended Data Fig. 1b-c**).

We next generated mutated pseudoviruses carrying S protein with mutations N501Y, A570D and the H69/V70 deletion. We observed no reduction in the ability of sera from vaccinees to inhibit either WT or mutant virus (**Extended Data Fig. 2**). In fact, we observed that vaccine sera displayed higher neutralizing activity against the N501Y, A570D and H69/V70 deletion mutant relative to WT virus. Next, we then tested a panel of sera from 11 recovered individuals and found that these sera also neutralised both wild type and the mutated viruses similarly (**Extended Data Fig. 3**). The findings for vaccine sera may be related to a potential allosteric effect of **Δ**H69/V70 that might enhance neutralization by antibodies targeting cryptic sites on the S, such as the RBD site II (also named as class 4 site).

We then generated the full set of eight mutations in the S protein present in B.1.1.7 variant (**Fig. 1b** and **Table 1**), **Δ**H69/V70, **Δ**144, N501Y and A570D in the S_1 subunit and P681H, T716I, S982A and D1118H in the S_2 subunit. All constructs also contained D614G. We found that among 15 individuals with neutralisation activity three weeks after receiving a single dose of the the BNT162b2 mRNA vaccine, 10 showed evidence of reduction in efficacy of antibodies against the B.1.1.7 mutant (fold change >3) (**Fig. 1c-d**). The highest fold change was approximately 6 and the median fold change was 3.85 (IQR 2.68-5.28). Amongst sera from 7 recovered individuals, only 2 demonstrated reduced potency against B.1.1.7 (**Fig. 1e-h** and **Extended Data Fig. 4**).

B.1.1.7 variant escapes from NTD- and RBM-specific mAb-mediated neutralization.

To investigate the role of the full set of mutations in NTD, RBD and S2 present in the B.1.1.7 variant, we tested 61 mAbs isolated from 15 individuals that recovered from WT SARS-CoV-2 infection with an *in-vitro* pseudotyped neutralization assay using VeroE6 target cells expressing TMPRSS2 (**Extended Data Table 1**). We found that 20 out of 61 (32.8%) mAbs

showed a greater than 2-fold loss of neutralizing activity of B.1.1.7 variant compared to WT SARS-CoV-2 (**Fig. 2a,b** and **Extended Data Fig. 5**). Remarkably, the B.1.1.7 mutant virus was found to fully escape neutralization by 7 out of 10 NTD-targeting mAbs (70%), and partial escape from additional 2 mAbs (20%) (**Fig. 2c**). We previously showed that the deletion of residue 144 abrogates binding by 4 out of 6 NTD-specific mAbs tested, possibly accounting for viral neutralization escape by most NTD-specific antibodies[22]. Of the 29 RBM-targeting mAbs, 5 (17.2%) showed more then 100-fold decrease in B.1.1.7 neutralization, and additional 6 mAbs (20.7%) had a partial 2-to-10-fold reduction (**Fig. 2d**). Finally, all RBD-specific non-RBM-targeting mAbs tested fully retained B.1.1.7 neutralizing activity (**Fig. 2e**).

To address the role of B.1.1.7 N501Y mutation in the neutralization escape from RBM-specific antibodies, we tested the binding of 51 RBD-specific mAbs to WT and N501Y mutant RBD by biolayer interferometry (**Fig. 2f** and **Extended Data Fig. 6**). The 5 RBM-specific mAbs that failed to neutralize B.1.1.7 variant (**Fig. 2d**) showed a complete loss of binding to N501Y RBD mutant (**Fig. 2g, h**), demonstrating a critical role for this mutation as an escape mechanism for RBM-targeting mAbs.

The decreased neutralizing activity of the immune sera from vaccinees and convalescent patients against B.1.1.7, but not against **Δ**69/70-501Y-570D mutant (**Fig. 1** and **Extended Data Fig. 2**), could be the result of a loss of neutralizing activity of both RBD- and NTD-targeting antibodies, and suggests that the key mutations driving polyclonal escape are **Δ**144 and N501Y.

SARS-CoV-2 B.1.1.7 binds human ACE2 with higher affinity than WT

SARS-CoV-2 and SARS-CoV enter host cells through binding of the S glycoprotein to ACE2[1,23]. Previous studies showed that the binding affinity of SARS-CoV for human ACE2 correlated with the rate of viral replication in distinct species, transmissibility and disease severity [24-26]. To understand the potential contribution of receptor interaction to infectivity, we set out to evaluate the influence of the B.1.1.7 RBD substitution N501Y on receptor engagement. We used biolayer interferometry to study binding kinetics and affinity of the purified human ACE2 ectodomain (residues 1-615) to immobilized biotinylated SARS-CoV-2 B.1.1.7 or WT RBDs. We found that ACE2 bound to the B.1.1.7 RBD with an affinity of 22 nM compared to 133 nM for the WT RBD **(Extended Data Fig. 7)**, in agreement with our previous deep-mutational scanning measurements using dimeric ACE2[27]. Although ACE2 bound with comparable on-rates to both RBDs, the observed dissociation rate constant was slower for B.1.1.7 than for the WT RBD **(Table 2)**. Enhanced binding of the B.1.1.7 RBD to

human ACE2 resulting from the N501Y mutation might participate to the efficient ongoing transmission of this newly emerged SARS-CoV-2 lineage, and possibly reduced opportunity for antibody binding.

Further loss of neutralization of vaccine-elicited antibodies against a B.1.1.7 Spike carrying E484K mutation

E484K as a lone Spike mutation is present in the UK (https://www.cogconsortium.uk/wp-content/uploads/2021/01/Report-2_COG-UK_SARS-CoV-2-Mutations.pdf). Given the inevitability of E484K emerging on the background of B.1.1.7, we generated data on the potency of vaccine sera against this combination. When testing B.1.1.7 with E484K against vaccine sera from five individuals, we observed a significant additional loss of neutralising activity (**Fig. 3**).

Discussion

Serum neutralizing activity is a correlate of protection for other respiratory viruses, including influenza[28] and respiratory syncytial virus where prohylaxis with monoclonal antibodies has been used in at-risk groups[29,30]. Neutralising antibody titres appeared to be highly correlated with vaccine protection against SARS-CoV-2 rechallenge in non-human primates, and importantly, there was no correlation between T cell responses (as measured by ELISPOT) and protection[31]. Moreover, passive transfer of purified polyclonal IgGs from convalescent macaques protected naïve macaques against subsequent SARS-CoV-2 challenge[32]. Coupled with multiple reports of re-infection, there has therefore been significant attention placed on virus neutralisation.

This is the first study reporting on the neutralisation escape from sera collected after one dose of the BNT162b2 vaccine in individuals. The participants of this study had a median age of over 80, in line with the targeting of this age group in the initial rollout of the vaccination campaign in the UK. Participants showed similar neutralising activity against wild type pseudovirus as in the phase I/II study, with geometric mean titres of 24 and 29, respectively[12]. The three mutations in S (N501Y, A570D, **Δ**H69/V70) did not appear to impact neutralisation in a pseudovirus assay. However, we demonstrated that a pseudovirus bearing S protein with the full set of mutations present in the B.1.1.7 variant (i.e., **Δ**H69/V70, **Δ**144, N501Y, A570D, P681H, T716I, S982A, D1118H) did result in reduced neutralisation by sera from vaccinees. A reduction in neutralization titres from mRNA-elicited antibodies in volunteers who received two doses (using both mRNA-1273 and BNT162b2 vaccines) was also observed by Wang et al.[33] using pseudoviruses carrying the N501Y mutation. Another study reported on a modest and not significant (average 1.2 fold) reduction of neutralization against the B.1.1.7 variant in sera from individuals vaccinated with two doses of mRNA-1273[34]. The level of neutralizing antibodies observed in both of these studies was approximately one log higher than the one observed in the cohort of vaccinees described in this study. This may be related to the older age of the individuals from this study as well as to the fact that these were exposed to only one dose of the BNT162b2 vaccine. In general, it is expected that the effect of mutations on the neutralization by polyclonal serum antibodies might be more prominent on low-titre in contrast to high-titre sera. It is important to study virus neutralisation at lower serum neutralisation titres because decline in neutralisation titres over time is expected to occur following vaccination.

The reduced neutralizing activity observed with polyclonal antibodies elicited by mRNA vaccines observed in this study and in Wang et al.[33] is further supported by the loss of neutralizing activity observed with human mAbs directed to both RBD and, to a major extent, to NTD. In the study by Wang et al., 6 out 17 RDB-specific mAbs isolated from mRNA-1273 vaccinated individuals showed more than 100-fold neutralization loss against N501Y mutant, a finding that is consistent with the loss of neutralization by 5 out 29 RBM-specific mAbs described in this study.

Multiple variants, including the 501Y.V2 and B.1.1.7 lineages, harbor multiple mutations as well as deletions in NTD, most of which are located in a site of vulnerability that is targeted by all known NTD-specific neutralizing antibodies[22]. The role of NTD-specific neutralizing antibodies might be under-estimated, in part by the use of neutralization assays based on target cells over-expressing ACE2 receptor. NTD-specific mAbs were suggested to interfere with viral entry based on other accessory receptors, such as DC-SIGN and L-SIGN[35], and their neutralization potency was found to be dependent on different in vitro culture conditions[22]. The observation that 9 out of 10 NTD-specific neutralizing antibodies failed to show a complete or near-complete loss of sneutralizing activity against B.1.1.7 indicates that this new variant may have evolved also to escape from this class of antibodies, that may have a yet unrecognized role in protective immunity. Wibmer et al.[36] have also recently reported the loss of neutralization of 501Y.V2 by the NTD-specific mAb 4A8, likely driven by the R246I mutation. This result is in line with the lack of neutralization of B.1.1.7 by 4A8 mAb observed in this study, likely caused by **Δ**144 due to loss of binding[22]. Finally, the role of NTD mutations (in particular, L18F, **Δ**242-244 and R246I) was further supported by the marked loss of neutralization observed by Wibmer et al.[36] against 501Y.V2 compared to the chimeric virus carrying only the RBD mutations K417N, E484K and N501Y. Taken together, the presence of multiple escape mutations in NTD is supportive of the hypothesis that this region of the Spike, in addition to RBM, is also under immune pressure.

E484K as a lone Spike mutation is present in the UK (https://www.cogconsortium.uk/wp-content/uploads/2021/01/Report-2_COG-UK_SARS-CoV-2-Mutations.pdf). It is inevitable that E484K will emerge in the background of B.1.1.7 and we therefore generated data on the potency of vaccine sera against this combination. E484K has been shown to impact neutralisation by monoclonal antibodies or convalescent sera, especially in combination with N501Y and K417N[16,37-39]. Here we show further reduction

neutralisation titers by vaccine sera when E484K is present alongside the B.1.1.7 S mutations. Consistent with our findings, Wu and co-authors[34] have shown that variants carrying the E484K mutation resulted in 3-to-6 fold reduction in neutralization by sera from mRNA-1273 vaccinated individuals.

Our study was limited by relatively small sample size. Although the Spike pseudotyping system has been shown to faithfully represent full length infectious virus, there may be determinants outside the S that influence escape from antibody neutralization either directly or indirectly in a live replication competent system. On the other hand live virus systems allow replication and therefore mutation to occur, and rigorous sequencing at multiple steps is needed.

Amidst high transmission in many parts of the world, vaccines are a key part of a long term strategy to bring SARS-CoV-2 under control. Our data suggest that vaccine escape will be inevitable in the future, and should be mitigated by designing next generation vaccines with mutated S sequences and using alternative viral antigens. Currently however, vaccines are likely to contribute controlling SARS-CoV-2 infections in the short term.

Acknowledgements

We would like to thank Cambridge University Hospitals NHS Trust Occupational Health Department. We would also like to thank the NIHR Cambridge Clinical Research Facility and staff at CUH and. We would like to thank Eleanor Lim and Georgina Okecha. We thank Dr James Voss for the kind gift of HeLa cells stably expressing ACE2. RKG is supported by a Wellcome Trust Senior Fellowship in Clinical Science (WT108082AIA). LEM is supported by a Medical Research Council Career Development Award (MR/R008698/1). SAK is supported by the Bill and Melinda Gates Foundation via PANGEA grant: OPP1175094. DAC is supported by a Wellcome Trust Clinical PhD Research Fellowship. KGCS is the recipient of a Wellcome Investigator Award (200871/Z/16/Z). This research was supported by the National Institute for Health Research (NIHR) Cambridge Biomedical Research Centre, the Cambridge Clinical Trials Unit (CCTU), and the NIHR BioResource. The views expressed are those of the authors and not necessarily those of the NIHR or the Department of Health and Social Care. JAGB is supported by the Medical Research Council (MC_UP_1201/16). IATM is funded by a SANTHE award.

Author contributions

Conceived study: D.C., RKG, DAC. Designed study and experiments: RKG, DAC, LEM, JB, MW, JT, LCG, GBM, RD, BG, NK, AE, M.P., D.V., L.P., A.D.M, J.B., D.C. Performed experiments: BM, DAC, RD, IATMF, LCG, GBM. Interpreted data: RKG, DAC, BM, RD, IATMF, LEM, JB, KGCS. A.D.M., J.B. and C.S.F. carried out pseudovirus neutralization assays. D.P. produced pseudoviruses. M.S.P., L.P., D.V. and D.C. designed the experiments. A.C.W., N.S. and S.J. expressed and purified the proteins. K.C., S.J. and E.C. sequenced and expressed antibodies. E.C. and K.C. performed mutagenesis for mutant expression plasmids. A.C.W. M.A.T., J.E.B., and S.B. performed binding assays. A.R., A.F.P and C.G contributed to donor's recruitment and sample collection related to mAbs isolation. H.W.V., G.S., A.L., D.V., L.P. and D.C. analyzed the data and prepared the manuscript with input from all authors.

Competing interests

A.D.M., J.B., D.P., C.S.F., S.B., K.C., N.S., E.C., G.S., S.J., A.L., H.W.V., M.S.P., L.P. and D.C. are employees of Vir Biotechnology and may hold shares in Vir Biotechnology. H.W.V. is a founder of PierianDx and Casma Therapeutics. Neither company provided funding for this work or is performing related work. D.V. is a consultant for Vir Biotechnology Inc. The Veesler laboratory has received a sponsored research agreement from Vir Biotechnology Inc. The remaining authors declare that the research was conducted in the absence of any commercial or financial relationships that could be construed as a potential conflict of interest. RKG has received consulting fees from UMOVIS Lab, Gilead and ViiV.

MATERIALS AND METHODS

Participant recruitment and ethics

Participants who had received the first dose of vaccine and individuals with COVID-19 were consented into the Covid-19 cohort of the NIHR Bioresource. The study was approved by the East of England – Cambridge Central Research Ethics Committee (17/EE/0025).

SARS-CoV-2 serology by multiplex particle-based flow cytometry (Luminex):

Recombinant SARS-CoV-2 N, S and RBD were covalently coupled to distinct carboxylated bead sets (Luminex; Netherlands) to form a 3-plex and analyzed as previously described (Xiong et al. 2020). Specific binding was reported as mean fluorescence intensities (MFI).

Recombinant expression of SARS-CoV-2-specific mAbs.

Human mAbs were isolated from plasma cells or memory B cells of SARS-CoV-2 immune donors, as previously described [40-42]. Recombinant antibodies were expressed in ExpiCHO cells at 37°C and 8% CO_2. Cells were transfected using ExpiFectamine. Transfected cells were supplemented 1 day after transfection with ExpiCHO Feed and ExpiFectamine CHO Enhancer. Cell culture supernatant was collected eight days after transfection and filtered through a 0.2 µm filter. Recombinant antibodies were affinity purified on an ÄKTA xpress FPLC device using 5 mL HiTrap™ MabSelect™ PrismA columns followed by buffer exchange to Histidine buffer (20 mM Histidine, 8% sucrose, pH 6) using HiPrep 26/10 desalting columns

Generation of S mutants

Amino acid substitutions were introduced into the D614G pCDNA_SARS-CoV-2_S plasmid as previously described[43] using the QuikChange Lightening Site-Directed Mutagenesis kit, following the manufacturer's instructions (Agilent Technologies, Inc., Santa Clara, CA). Sequences were checked by Sanger sequencing.

Preparation of B.1.1.7 SARS-CoV-2 S glycoprotein-encoding-plasmid used to produce SARS-CoV-2-MLV based on overlap extension PCR. Briefly, a modification of the overlap extension PCR protocol[44] was used to introduce the nine mutations of the B.1.1.7 lineage in the SARS-CoV-2 S gene. In a first step, 9 DNA fragments with overlap sequences were amplified by PCR from a plasmid (phCMV1, Genlantis) encoding the full-length SARS-CoV-2 S gene (BetaCoV/Wuhan-Hu-1/2019, accession number mn908947). The mutations (del-69/70, del-144, N501Y, A570D, D614G, P681H, S982A, T716I and D1118H) were introduced by amplification with primers with similar Tm. Deletion of the C-terminal 21 amino acids was introduced to increase surface expression of the recombinant S[45]. Next, 3 contiguous overlapping fragments were fused by a first overlap PCR (step 2) using the utmost external primers of each set, resulting in 3 larger fragments with overlapping sequences. A final overlap PCR (step 3) was performed on the 3 large fragments using the utmost external primers to amplify the full-length S gene and the flanking sequences including the restriction sites KpnI and NotI. This fragment was digested and cloned into the expression plasmid phCMV1. For all PCR reactions the Q5 Hot Start High fidelity DNA polymerase was used (New England Biolabs Inc.), according to the manufacturer's instructions and adapting the elongation time to the size of the amplicon. After each PCR step the amplified regions were separated on agarose gel and purified using Illustra GFX™ PCR DNA and Gel Band Purification Kit (Merck KGaA).

Pseudotype virus preparation

Viral vectors were prepared by transfection of 293T cells by using Fugene HD transfection reagent (Promega). 293T cells were transfected with a mixture of 11ul of Fugene HD, 1µg of pCDNAΔ19Spike-HA, 1ug of p8.91 HIV-1 gag-pol expression vector[46,47], and 1.5µg of pCSFLW (expressing the firefly luciferase reporter gene with the HIV-1 packaging signal). Viral supernatant was collected at 48 and 72h after transfection, filtered through 0.45um filter and stored at -80˚C. The 50% tissue culture infectious dose ($TCID_{50}$) of SARS-CoV-2 pseudovirus was determined using Steady-Glo Luciferase assay system (Promega).

Serum/plasma pseudotype neutralization assay

Spike pseudotype assays have been shown to have similar characteristics as neutralisation testing using fully infectious wild type SARS-CoV-2[20]. Virus neutralisation assays were performed on 293T cell transiently transfected with ACE2 and TMPRSS2 using SARS-CoV-2 Spike pseudotyped virus expressing luciferase[48]. Pseudotyped virus was incubated with serial dilution of heat inactivated human serum samples or sera from vaccinees in duplicate for 1h at 37˚C. Virus and cell only controls were also included. Then, freshly trypsinized 293T ACE2/TMPRSS2 expressing cells were added to each well. Following 48h incubation in a 5% CO_2 environment at 37°C, luminescence was measured using the Steady-Glo Luciferase assay system (Promega).

IFNγ FLUOROSPOT assays

Frozen PBMCs were rapidly thawed, and the freezing medium was diluted into 10ml of TexMACS media (Miltenyi Biotech), centrifuged and resuspended in 10ml of fresh media with 10U/ml DNase (Benzonase, Merck-Millipore via Sigma-Aldrich), PBMCs were incubated at 37°C for 1h, followed by centrifugation and resuspension in fresh media supplemented with 5% Human AB serum (Sigma Aldrich) before being counted. PBMCs were stained with 2ul of each antibody: anti-CD3-fluorescein isothiocyanate (FITC), clone UCHT1; anti-CD4-phycoerythrin (PE), clone RPA-T4; anti-CD8a-peridinin-chlorophyll protein - cyanine 5.5 (PerCP Cy5.5), clone RPA-8a (all BioLegend, London, UK), LIVE/DEAD Fixable Far Red Dead Cell Stain Kit (Thermo Fisher Scientific). PBMC phenotyping was performed on the BD Accuri C6 flow cytometer. Data were analysed with FlowJo v10 (Becton Dickinson, Wokingham, UK). 1.5 to 2.5 x 105 PBMCs were incubated

in pre-coated Fluorospot plates (Human IFNγ FLUOROSPOT (Mabtech AB, Nacka Strand, Sweden)) in triplicate with peptide mixes specific for Spike, Nucleocapsid and Membrane proteins of SARS-CoV-2 (final peptide concentration 1µg/ml/peptide, Miltenyi Biotech) and an unstimulated and positive control mix (containing anti-CD3 (Mabtech AB), Staphylococcus Enterotoxin B (SEB), Phytohaemagglutinin (PHA) (all Sigma Aldrich)) at 37ºC in a humidified CO2 atmosphere for 48 hours. The cells and medium were decanted from the plate and the assay developed following the manufacturer's instructions. Developed plates were read using an AID iSpot reader (Oxford Biosystems, Oxford, UK) and counted using AID EliSpot v7 software (Autoimmun Diagnostika GmbH, Strasberg, Germany). All data were then corrected for background cytokine production and expressed as SFU/Million PBMC or CD3 T cells.

MAbs pseudovirus neutralization assay

MLV-based SARS-CoV-2 S-glycoprotein-pseudotyped viruses were prepared as previously described (Pinto et al., 2020). HEK293T/17cells were cotransfected with a WT or B.1.1.7 SARS-CoV-2 Spike glycoprotein-encoding-plasmid, an MLV Gag-Pol packaging construct and the MLV transfer vector encoding a luciferase reporter using X-tremeGENE HP transfection reagent (Roche) according to the manufacturer's instructions. Cells were cultured for 72 h at 37°C with 5% CO_2 before harvesting the supernatant. VeroE6 stably expressing human TMPRSS2 were cultured in DMEM containing 10% FBS, 1% penicillin–streptomycin, 8 µg/mL puromycin and plated into 96-well plates for 16–24 h. Pseudovirus with serial dilution of mAbs was incubated for 1 h at 37°C and then added to the wells after washing 2 times with DMEM. After 2–3 h DMEM containing 20% FBS and 2% penicillin–streptomycin was added to the cells. Following 48-72 h of infection, Bio-Glo (Promega) was added to the cells and incubated in the dark for 15 min before reading luminescence with Synergy H1 microplate reader (BioTek). Measurements were done in duplicate and relative luciferase units were converted to percent neutralization and plotted with a non-linear regression model to determine IC50 values using GraphPad PRISM software (version 9.0.0).

Antibody binding measurements using bio-layer interferometry (BLI)

MAbs were diluted to 3 µg/ml in kinetic buffer (PBS supplemented with 0.01% BSA) and immobilized on Protein A Biosensors (FortéBio). Antibody-coated biosensors were incubated for 3 min with a solution containing 5 µg /ml of WT or N50Y SARS-CoV-2 RBD in kinetic buffer, followed by a 3-min dissociation step. Change in molecules bound to the biosensors

caused a shift in the interference pattern that was recorded in real time using an Octet RED96 system (FortéBio). The binding response over time was used to calculate the area under the curve (AUC) using GraphPad PRISM software (version 9.0.0).

Production of SARS-CoV-2 and B.1.1.7 receptor binding domains and human ACE2

The SARS-CoV-2 RBD (BEI NR-52422) construct was synthesized by GenScript into CMVR with an N-terminal mu-phosphatase signal peptide and a C-terminal octa-histidine tag (GHHHHHHHH) and an avi tag. The boundaries of the construct are N-$_{328}$RFPN$_{331}$ and $_{528}$KKST$_{531}$-C[49]. The B.1.1.7 RBD was synthesized by GenScript into pCMVR with the same boundaries and construct details with a mutation at N501Y. These plasmids were transiently transfected into Expi293F cells using Expi293F expression medium (Life Technologies) at 37°C 8% CO_2 rotating at 150 rpm. The cultures were transfected using PEI cultivated for 5 days. Supernatants were clarified by centrifugation (10 min at 4000xg) prior to loading onto a nickel-NTA column (GE). Purified protein was biotinylated overnight using BirA (Avidity) prior to SEC into PBS. Human ACE2-Fc (residues 1-615 with a C-terminal thrombin cleavage site and human Fc tag) were synthesized by Twist. Clarified supernatants were affinity purified using a Protein A column (GE LifeSciences) directly neutralized and buffer exchanged. The Fc tag was removed by thrombin cleavage in a reaction mixture containing 3 mg of recombinant ACE2-FC ectodomain and 10 μg of thrombin in 20 mM Tris-HCl pH8.0, 150 mM NaCl and 2.5 mM $CaCl_2$.The reaction mixture was incubated at 25°C overnight and re-loaded on a Protein A column to remove uncleaved protein and the Fc tag. The cleaved protein was further purified by gel filtration using a Superdex 200 column 10/300 GL (GE Life Sciences) equilibrated in PBS.

Protein affinity measurement using bio-layer interferometry

Biotinylated RBD (either WT or N501Y) were immobilized at 5 ng/uL in undiluted 10X Kinetics Buffer (Pall) to SA sensors until a load level of 1.1nm, A dilution series of either monomeric ACE2 or Fab in undiluted kinetics buffer starting at 1000-50nM was used for 300-600 seconds to determine protein-protein affinity. The data were baseline subtracted and the plots fitted using the Pall FortéBio/Sartorius analysis software (version 12.0). Data were plotted in Prism.

Table 1: Vaccinee Participants and serum neutralisation data; ID50 (inhibitory dilution) is the dilution required to achieve neutralisation of 50% infection by the virus. fold change (FC). NA: not available.

ID	Age	Mean ID50 (SD) WT	Fold Change Δ69/70 501Y 570D	Fold Change B.1.1.7 Spike mutations
1	60-65	34 (21)	0.435739	1.78
2	80-85	105 (62)	1.041735	2.18
3	40-45	93 (73)	0.32497	2.68
4	85-90	28 (15)	1.55961	-
5	25-30	27 (7)	0.386996	4.80
6	35-40	9 (0)	0.183133	4.46
7	80-85	27 (11)	0.383294	5.83
8	80-85	1 (0)	-	-
9	55-60	834 (658)	0.58253	2.88
10	85-90	1 (0)	-	-
11	80-85	2 (1)	-	-
12	80-85	3 (2)	-	-
13	80-85	4 (1)	-	-
14	85-90	41 (16)	0.468458	4.07025411
15	75-80	233 (104)	NA	6.12008534
16	80-85	1 (0)	-	-
17	80-85	1 (0)	-	-
18	85-90	723 (385)	0.674522	3.62182971
19	85-90	29 (7)	0.230936	5.41319667
20	80-85	63 (44)	0.538738	3.85473562
22	55-60	41 (17)	0.395114	5.27833669
25	60-65	52 (12)	0.808271	2.34132055
28	80-82	3449 (2489)	0.60931	3.17481581

Table 2. Kinetic analysis of human ACE2 binding to SARS-CoV-2 B.1.1.7 and Wuhan-1 RBDs by biolayer interferometry. Values reported represent the global fit to the data shown in Extended Data Fig. 7.

		SARS-CoV-2 RBD WT	SARS-CoV-2 RBD B.1.1.7
K_D (nM)		133	22
k_{on} ($M^{-1}.s^{-1}$)	hACE2	$1.3*10^5$	$1.4*10^5$

k_{off} (s^{-1})		$1.8*10^{-2}$	$3*10^{-3}$

Extended Data Table 1. Neutralization, V gene usage and other properties of tested mAbs.

mAb	Domain (site)	VH usage (% id.)	Source (DSO)	IC50 WT (ng/ml)	IC50 B.1.1.7 (ng/ml)	ACE2 blocking	SARS-CoV	Escape residues	Ref.
4A8	NTD (i)	1-24	N/A	38	-	Neg.	-	S12P; C136Y; Y144del; H146Y; K147T; R246A	[50]
S2L26	NTD (i)	1-24 (97.2)	Hosp. (52)	70	-	Neg.	-	N/A	[22]
S2L50	NTD (i)	4-59 (95.4)	Hosp. (52)	264	50	Neg.	-	N/A	[22]
S2M28	NTD (i)	3-33 (97.6)	Hosp. (46)	295	12'207	Neg.	-	P9S/Q; S12P; C15F/R; L18P; Y28C; A123T; C136Y; G142D; Y144del; K147Q/T; R246G; P251L; G252C	[22]
S2X107	NTD (i)	4-38-2 (97)	Sympt. (75)	388	-	Neg.	-	N/A	[22]
S2X124	NTD (i)	3-30 (99)	Sympt. (75)	221	-	Neg.	-	N/A	[22]
S2X158	NTD (i)	1-24 (96.3)	Sympt. (75)	56	-	Neg.	-	N/A	[22]
S2X28	NTD (i)	3-30 (97.9)	Sympt. (48)	1'399	-	Neg.	-	P9S; S12P; C15W; L18P; C136G/Y; F140S; L141S; G142C/D; Y144C/N; K147T/Q/E; R158G; L244S; R246G	[22]
S2X303	NTD (i)	2-5 (95.9)	Sympt. (125)	69	-	Neg.	-	N/A	[22]
S2X333	NTD (i)	3-33 (96.5)	Sympt. (125)	66	-	Neg.	-	P9L; S12P; C15S/Y; L18P; C136G/Y; F140C; G142D; K147T	[22]
S2D106	RBD (I/RBM)	1-69 (97.2)	Hosp. (98)	27	20	Strong	-	N/A	[8]
S2D19	RBD (I/RBM)	4-31 (99.7)	Hosp. (49)	128	75'200	Moderate	-	N/A	[8]
S2D32	RBD (I/RBM)	3-49 (98.3)	Hosp. (49)	26	11	Strong	-	N/A	[8]
S2D65	RBD (I/RBM)	3-9 (96.9)	Hosp. (49)	24	12	Weak	-	N/A	[8]
S2D8	RBD (I/RBM)	3-23 (96.5)	Hosp. (49)	27	58'644	Strong	-	N/A	[8]
S2D97	RBD (I/RBM)	2-5 (96.9)	Hosp. (98)	20	17	Weak	-	N/A	[8]
S2E11	RBD (I/RBM)	4-61 (98.3)	Hosp. (51)	27	16	Weak	-	N/A	[8]
S2E12	RBD (I/RBM)	1-58 (97.6)	Hosp. (51)	27	31	Strong	-	G476S (3x)	[8,51]
S2E13	RBD (I/RBM)	1-18 (96.2)	Hosp. (51)	34	77	Strong	-	N/A	[8]
S2E16	RBD (I/RBM)	3-30 (98.3)	Hosp. (51)	36	38	Strong	-	N/A	[8]
S2E23	RBD (I/RBM)	3-64 (96.9)	Hosp. (51)	139	180	Strong	-	N/A	[8]
S2H14	RBD (I/RBM)	3-15 (100)	Sympt. (17)	460	64'463	Weak	-	N/A	[8,52]
S2H19	RBD (I/RBM)	3-15 (98.6)	Sympt. (45)	239	-	Weak	-	N/A	[8]
S2H58	RBD (I/RBM)	1-2 (97.9)	Sympt. (45)	27	14	Strong	-	N/A	[8]
S2H7	RBD (I/RBM)	3-66 (98.3)	Sympt. (17)	492	573	Weak	-	N/A	[8]
S2H70	RBD (I/RBM)	1-2 (99)	Sympt. (45)	147	65	Weak	-	N/A	[8]
S2H71	RBD (I/RBM)	2-5 (99)	Sympt. (45)	36	9	Moderate	-	N/A	[8]
S2M11	RBD (I/RBM)	1-2 (96.5)	Hosp. (46)	11	4	Weak	-	Y449N; L455F; E484K; E484Q; F490L; F490S; S494P	[8,51]

S2N12	RBD (I/RBM)	4-39 (97.6)	Hosp. (51)	76	40	Strong	-	N/A	[8]
S2N22	RBD (I/RBM)	3-23 (96.5)	Hosp. (51)	32	21	Strong	-	N/A	[8]
S2N28	RBD (I/RBM)	3-30 (97.2)	Hosp. (51)	72	21	Strong	-	N/A	[8]
S2X128	RBD (I/RBM)	1-69-2 (97.6)	Sympt. (75)	50	112	Strong	-	N/A	[8]
S2X16	RBD (I/RBM)	1-69 (97.6)	Sympt. (48)	45	103	Strong	-	N/A	[8]
S2X192	RBD (I/RBM)	1-69 (96.9)	Sympt. (75)	326	-	Weak	-	N/A	[8]
S2X227	RBD (I/RBM)	1-46 (97.9)	Sympt. (75)	26	14	Strong	-	N/A	
S2X246	RBD (I/RBM)	3-48 (96.2)	Sympt. (75)	35	30	Strong	-	N/A	
S2X30	RBD (I/RBM)	1-69 (97.9)	Sympt. (48)	32	53	Strong	-	N/A	[8]
S2X324	RBD (I/RBM)	2-5 (97.3)	Sympt. (125)	8	23	Strong	-	N/A	
S2X58	RBD (I/RBM)	1-46 (99)	Sympt. (48)	32	47	Strong	-	N/A	[8]
S2H90	RBD (II)	4-61 (96.6)	Sympt. (81)	77	32	Strong	+	N/A	[8]
S2H94	RBD (II)	3-23 (93.4)	Sympt. (81)	123	144	Strong	+	N/A	[8]
S2H97	RBD (V)	5-51 (98.3)	Sympt. (81)	513	248	Weak	+	N/A	
S2K15	RBD (II)	2-26 (99.3)	Sympt. (87)	361	235	0	+	N/A	
S2K21	RBD (II)	3-33 (96.2)	Sympt. (118)	201	189	0	+	N/A	
S2K30	RBD (II)	1-2 (97.2)	Sympt. (87)	185	134	0	+	N/A	
S2K63v2	RBD (II)	3-30-3 (95.6)	Sympt. (118)	144	215	0	+	N/A	
S2L17	RBD (?)	5-10-1 (98.3)	Hosp. (51)	313	127	Moderate	+	N/A	[8]
S2L37	RBD (II)	3-13 (98.3)	Hosp. (51)	14'370	824	Moderate	+	N/A	
S2L49	RBD (?)	3-30 (97.9)	Hosp. (51)	24	32	Neg.	+	N/A	[8]
S2X259	RBD (IIa)	1-69 (94.1)	Sympt. (75)	145	91	Moderate	+	N/A	
S2X305	RBD (?)	1-2 (95.1)	Sympt. (125)	34	21	Strong	-	N/A	
S2X35	RBD (IIa)	1-18 (98.6)	Sympt. (48)	140	143	Strong	+	N/A	[52]
S2X450	RBD (?)	2-26 (96.9)	Sympt. (271)	368	198	Strong	+	N/A	
S2X475	RBD (?)	3-21 (93.8)	Sympt. (271)	1'431	851	Strong	+	N/A	
S2X607	RBD (?)	3-66 (95.4)	Sympt. (271)	41	23	Strong	-	N/A	
S2X608	RBD (?)	1-33 (93.2)	Sympt. (271)	21	35	Strong	-	N/A	
S2X609	RBD (?)	1-69 (93.8)	Sympt. (271)	47	35	Strong	-	N/A	
S2X613	RBD (?)	1-2 (91.7)	Sympt. (271)	28	19	Strong	-	N/A	
S2X615	RBD (?)	3-11 (94.8)	Sympt. (271)	23	17	Strong	-	N/A	
S2X619	RBD (?)	1-69 (92.7)	Sympt. (271)	36	60	Strong	-	N/A	
S2X620	RBD (?)	3-53 (95.1)	Sympt. (271)	34	45	Strong	-	N/A	

id., identity. DSO, days after symptom onset. * as described in Piccoli et al and McCallum et al. N/A, not available; -, not neutralizing

References

1 Zhou, P. *et al.* A pneumonia outbreak associated with a new coronavirus of probable bat origin. *Nature* **579**, 270-273, doi:10.1038/s41586-020-2012-7 (2020).

2 Davies, N. G. *et al.* Estimated transmissibility and severity of novel SARS-CoV-2 Variant of Concern 202012/01 in England. *medRxiv*, 2020.2012.2024.20248822, doi:10.1101/2020.12.24.20248822 (2020).

3 Volz, E. *et al.* Transmission of SARS-CoV-2 Lineage B.1.1.7 in England: Insights from linking epidemiological and genetic data. *medRxiv*, 2020.2012.2030.20249034, doi:10.1101/2020.12.30.20249034 (2021).

4 Korber, B. *et al.* Tracking Changes in SARS-CoV-2 Spike: Evidence that D614G Increases Infectivity of the COVID-19 Virus. *Cell* **182**, 812-827 e819, doi:10.1016/j.cell.2020.06.043 (2020).

5 Yurkovetskiy, L. *et al.* Structural and Functional Analysis of the D614G SARS-CoV-2 Spike Protein Variant. *Cell* **183**, 739-751 e738, doi:10.1016/j.cell.2020.09.032 (2020).

6 Martinot, M. *et al.* Remdesivir failure with SARS-CoV-2 RNA-dependent RNA-polymerase mutation in a B-cell immunodeficient patient with protracted Covid-19. *Clin Infect Dis*, doi:10.1093/cid/ciaa1474 (2020).

7 Kemp, S. *et al.* Neutralising antibodies in Spike mediated SARS-CoV-2 adaptation. *medRxiv*, 2020.2012.2005.20241927, doi:10.1101/2020.12.05.20241927 (2020).

8 Thomson, E. C. *et al.* The circulating SARS-CoV-2 spike variant N439K maintains fitness while evading antibody-mediated immunity. *bioRxiv*, 1-49, doi:papers3://publication/doi/10.1101/2020.11.04.355842 (2020).

9 Baden, L. R. *et al.* Efficacy and Safety of the mRNA-1273 SARS-CoV-2 Vaccine. *N Engl J Med*, doi:10.1056/NEJMoa2035389 (2020).

10 Polack, F. P. *et al.* Safety and Efficacy of the BNT162b2 mRNA Covid-19 Vaccine. *N Engl J Med* **383**, 2603-2615, doi:10.1056/NEJMoa2034577 (2020).

11 Voysey, M. *et al.* Safety and efficacy of the ChAdOx1 nCoV-19 vaccine (AZD1222) against SARS-CoV-2: an interim analysis of four randomised controlled trials in Brazil, South Africa, and the UK. *Lancet* **397**, 99-111, doi:10.1016/S0140-6736(20)32661-1 (2021).

12 Mulligan, M. J. *et al.* Phase I/II study of COVID-19 RNA vaccine BNT162b1 in adults. *Nature* **586**, 589-593, doi:10.1038/s41586-020-2639-4 (2020).

13 Corbett, K. S. *et al.* SARS-CoV-2 mRNA Vaccine Development Enabled by Prototype Pathogen Preparedness. *bioRxiv*, 2020.2006.2011.145920, doi:10.1101/2020.06.11.145920 (2020).

14 Folegatti, P. M. *et al.* Safety and immunogenicity of the ChAdOx1 nCoV-19 vaccine against SARS-CoV-2: a preliminary report of a phase 1/2, single-blind, randomised controlled trial. *Lancet* **396**, 467-478, doi:10.1016/S0140-6736(20)31604-4 (2020).

15 Kemp, S. A. *et al.* Recurrent emergence and transmission of a SARS-CoV-2 Spike deletion ΔH69/V70. *bioRxiv*, 2020.2012.2014.422555, doi:10.1101/2020.12.14.422555 (2020).

16 Tegally, H. *et al.* Emergence and rapid spread of a new severe acute respiratory syndrome-related coronavirus 2 (SARS-CoV-2) lineage with multiple spike mutations in South Africa. *medRxiv*, 2020.2012.2021.20248640, doi:10.1101/2020.12.21.20248640 (2020).

17 Faria, N. R. *et al. Genomic characterisation of an emergent SARS-CoV-2 lineage in Manaus: preliminary findings*, <https://virological.org/t/genomic-characterisation-of-an-emergent-sars-cov-2-lineage-in-manaus-preliminary-findings/586> (2021).

18 Jackson, L. A. *et al.* An mRNA Vaccine against SARS-CoV-2 - Preliminary Report. *N Engl J Med* **383**, 1920-1931, doi:10.1056/NEJMoa2022483 (2020).

19 Walsh, E. E. *et al.* Safety and Immunogenicity of Two RNA-Based Covid-19 Vaccine Candidates. *New England Journal of Medicine* **383**, 2439-2450, doi:10.1056/NEJMoa2027906 (2020).

20 Schmidt, F. *et al.* Measuring SARS-CoV-2 neutralizing antibody activity using pseudotyped and chimeric viruses. 2020.2006.2008.140871, doi:10.1101/2020.06.08.140871 %J bioRxiv (2020).

21 Brouwer, P. J. M. *et al.* Potent neutralizing antibodies from COVID-19 patients define multiple targets of vulnerability. *Science* **369**, 643-650, doi:10.1126/science.abc5902 (2020).

22 McCallum, M. *et al.* N-terminal domain antigenic mapping reveals a site of vulnerability for SARS-CoV-2. *bioRxiv*, doi:10.1101/2021.01.14.426475 (2021).

23 Walls, A. C. *et al.* Structure, Function, and Antigenicity of the SARS- CoV-2 Spike Glycoprotein. *Cell* **181**, 281-292.e286, doi:papers3://publication/doi/10.1016/j.cell.2020.02.058 (2020).

24 Guan, Y. *et al.* Isolation and characterization of viruses related to the SARS coronavirus from animals in southern China. *Science* **302**, 276-278, doi:10.1126/science.1087139 (2003).

25 Li, W. *et al.* Efficient replication of severe acute respiratory syndrome coronavirus in mouse cells is limited by murine angiotensin-converting enzyme 2. *J Virol* **78**, 11429-11433, doi:10.1128/JVI.78.20.11429-11433.2004 (2004).

26 Li, W. *et al.* Receptor and viral determinants of SARS-coronavirus adaptation to human ACE2. *EMBO J* **24**, 1634-1643, doi:10.1038/sj.emboj.7600640 (2005).

27 Starr, T. N. *et al.* Deep Mutational Scanning of SARS-CoV-2 Receptor Binding Domain Reveals Constraints on Folding and ACE2 Binding. *Cell* **182**, 1295-1310 e1220, doi:10.1016/j.cell.2020.08.012 (2020).

28 Verschoor, C. P. *et al.* Microneutralization assay titres correlate with protection against seasonal influenza H1N1 and H3N2 in children. *PloS one* **10**, e0131531, doi:10.1371/journal.pone.0131531 (2015).

29 Kulkarni, P. S., Hurwitz, J. L., Simoes, E. A. F. & Piedra, P. A. Establishing Correlates of Protection for Vaccine Development: Considerations for the Respiratory Syncytial Virus Vaccine Field. *Viral Immunol* **31**, 195-203, doi:10.1089/vim.2017.0147 (2018).

30 Goddard, N. L., Cooke, M. C., Gupta, R. K. & Nguyen-Van-Tam, J. S. Timing of monoclonal antibody for seasonal RSV prophylaxis in the United Kingdom. *Epidemiol Infect* **135**, 159-162, doi:10.1017/S0950268806006601 (2007).

31 Mercado, N. B. *et al.* Single-shot Ad26 vaccine protects against SARS-CoV-2 in rhesus macaques. *Nature* **586**, 583-588, doi:10.1038/s41586-020-2607-z (2020).

32 McMahan, K. *et al.* Correlates of protection against SARS-CoV-2 in rhesus macaques. *Nature*, doi:10.1038/s41586-020-03041-6 (2020).

33 Wang, Z. *et al.* mRNA vaccine-elicited antibodies to SARS-CoV-2 and circulating variants. *bioRxiv*, doi:10.1101/2021.01.15.426911 (2021).

34 Wu, K. *et al.* mRNA-1273 vaccine induces neutralizing antibodies against spike mutants from global SARS-CoV-2 variants. *bioXriv*, doi:10.1101/2021.01.25.427948 (2021).
35 Soh, W. T. *et al.* The N-terminal domain of spike glycoprotein mediates SARS-CoV-2 infection by associating with L-SIGN and DC-SIGN. 1-30, doi:papers3://publication/doi/10.1101/2020.11.05.369264 (2020).
36 Wibmer, C. K. *et al.* SARS-CoV-2 501Y.V2 escapes neutralization by South African COVID-19 donor plasma. *bioRxiv*, doi:10.1101/2021.01.18.427166 (2021).
37 Greaney, A. J. *et al.* Comprehensive mapping of mutations to the SARS-CoV-2 receptor-binding domain that affect recognition by polyclonal human serum antibodies. *bioRxiv*, 2020.2012.2031.425021, doi:10.1101/2020.12.31.425021 (2021).
38 Greaney, A. J. *et al.* Complete mapping of mutations to the SARS-CoV-2 spike receptor-binding domain that escape antibody recognition. *Cell Host & Microbe* (2020).
39 Weisblum, Y. *et al.* Escape from neutralizing antibodies by SARS-CoV-2 spike protein variants. *Elife* **9**, e61312, doi:10.7554/eLife.61312 (2020).
40 Corti, D. *et al.* A neutralizing antibody selected from plasma cells that binds to group 1 and group 2 influenza A hemagglutinins. *Science* **333**, 850-856, doi:10.1126/science.1205669 (2011).
41 Pinto, D. *et al.* Cross-neutralization of SARS-CoV-2 by a human monoclonal SARS-CoV antibody. *Nature* **583**, 290-295, doi:10.1038/s41586-020-2349-y (2020).
42 Tortorici, M. A. *et al.* Ultrapotent human antibodies protect against SARS-CoV-2 challenge via multiple mechanisms. *Science*, doi:10.1126/science.abe3354 (2020).
43 Gregson, J. *et al.* HIV-1 viral load is elevated in individuals with reverse transcriptase mutation M184V/I during virological failure of first line antiretroviral therapy and is associated with compensatory mutation L74I. *Journal of Infectious Diseases* (2019).
44 Forloni, M., Liu, A. Y. & Wajapeyee, N. Creating Insertions or Deletions Using Overlap Extension Polymerase Chain Reaction (PCR) Mutagenesis. *Cold Spring Harb Protoc* **2018**, doi:10.1101/pdb.prot097758 (2018).
45 Case, J. B. *et al.* Neutralizing Antibody and Soluble ACE2 Inhibition of a Replication-Competent VSV-SARS-CoV-2 and a Clinical Isolate of SARS-CoV-2. *Cell Host Microbe* **28**, 475-485 e475, doi:10.1016/j.chom.2020.06.021 (2020).
46 Naldini, L., Blomer, U., Gage, F. H., Trono, D. & Verma, I. M. Efficient transfer, integration, and sustained long-term expression of the transgene in adult rat brains injected with a lentiviral vector. *Proc Natl Acad Sci U S A* **93**, 11382-11388, doi:10.1073/pnas.93.21.11382 (1996).
47 Gupta, R. K. *et al.* Full length HIV-1 gag determines protease inhibitor susceptibility within in vitro assays. *AIDS* **24**, 1651 (2010).
48 Mlcochova, P. *et al.* Combined point of care nucleic acid and antibody testing for SARS-CoV-2 following emergence of D614G Spike Variant. *Cell Rep Med*, 100099, doi:10.1016/j.xcrm.2020.100099 (2020).
49 Walls, A. C. *et al.* Elicitation of Potent Neutralizing Antibody Responses by Designed Protein Nanoparticle Vaccines for SARS-CoV-2. *Cell* **183**, 1367-1382 e1317, doi:10.1016/j.cell.2020.10.043 (2020).

50 Chi, X. *et al.* A neutralizing human antibody binds to the N-terminal domain of the Spike protein of SARS-CoV-2. *Science*, eabc6952-6913, doi:papers3://publication/doi/10.1126/science.abc6952 (2020).

51 Tortorici, M. A. *et al.* Ultrapotent human antibodies protect against SARS-CoV-2 challenge via multiple mechanisms. *Science* **4**, eabe3354-3316, doi:papers3://publication/doi/10.1126/science.abe3354 (2020).

52 Piccoli, L. *et al.* Mapping neutralizing and immunodominant sites on the SARS-CoV-2 spike receptor-binding domain by structure-guided high-resolution serology. *Cell*, 1-55, doi:papers3://publication/doi/10.1016/j.cell.2020.09.037 (2020).

Figure 1

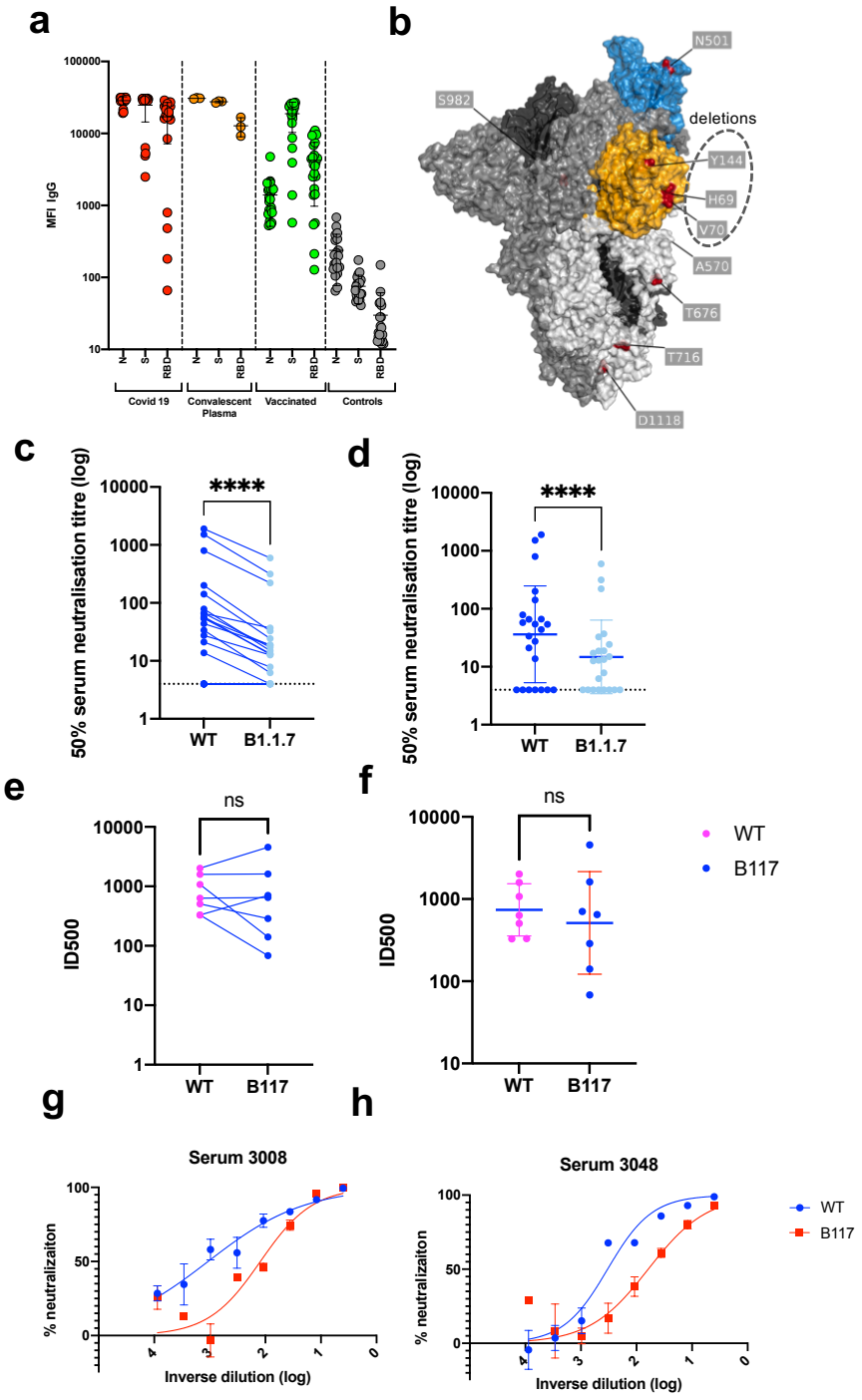

Figure 1. Neutralisation by sera against wild type and B.1.1.7 Spike mutant SARS-CoV-2 pseudotyped viruses. a, Serum IgG responses against N protein, Spike and the Spike Receptor Binding Domain (RBD) from 23 vaccinated participants (green), 20 recovered COVID-19 cases (red), 3 convalescent plasma units and 20 healthy controls (grey) as measured by a flow cytometry based Luminex assay. MFI, mean fluorescence intensity. **b,** Spike in open conformation with a single erect RBD (PDB: 6ZGG) in trimer axis vertical view with the locations of mutated residues highlighted in red spheres and labelled on the monomer with erect RBD. Vaccine (**c-d**) and convalescent sera (**e-f)** against WT and B.1.1.7 Spike mutant with N501Y, A570D, **Δ**H69/V70, **Δ**144/145, P681H, T716I, S982A and D1118H. **g-h,** neutralisation curves for serum from two convalescent individuals with reduced susceptibility to B.1.1.7 Spike mutant, means of technical replicates are plotted with error bars representing standard error of mean. Data are representative of 2 independent experiments.

Figure 2

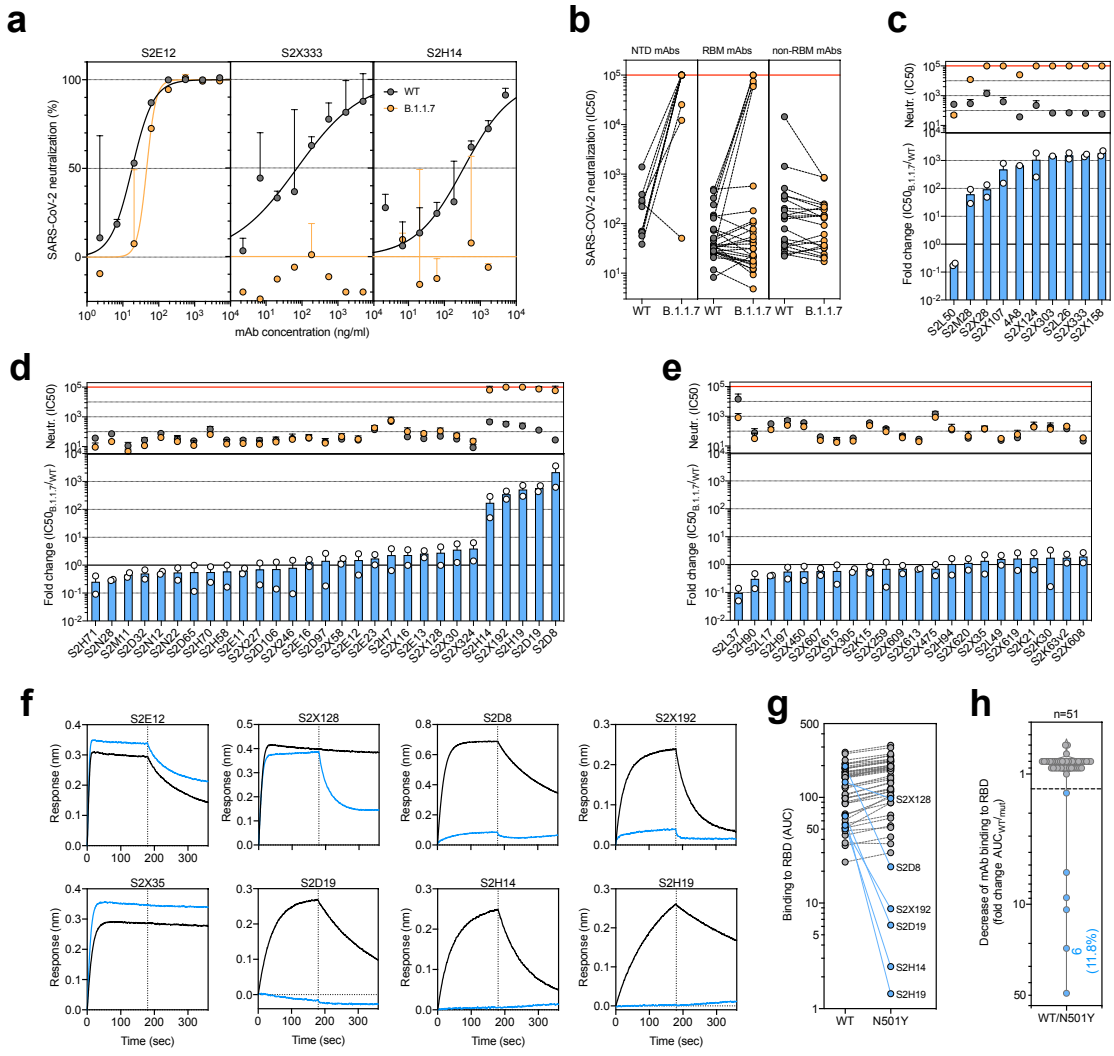

Figure 2. Neutralisation and binding by a panel of NTD- and RBD-specific mAbs against WT and B.1.1.7 SARS-CoV-2 viruses. a, Neutralisation of WT (black) and B.1.1.7 (orange) Spike pseudotyped SARS-CoV-2-MLV by 3 selected mAbs (S2E12, S2X333 and S2H14) from one representative experiment. Shown is the mean ± s.d. of 2 technical replicates. **b,** Neutralisation of WT and B.1.1.7 SARS-CoV-2-MLV by 61 mAbs targeting NTD (n=10), RBM (n=29) and non-RBM sites in the RBD (n=22). Shown are the mean IC50 values (ng/ml) of n=2 independent experiments. **c-e,** Neutralisation shown as mean IC50 values (upper panel) and mean fold change of B.1.1.7 relative to WT (lower panel) of NTD (c), RBM (d) and non-RBM (e) mAbs. Lower panel shows IC50 values from 2 independent experiments. **f-h,** Kinetics of binding of mAbs to WT (black) and N501Y (blue) RBD as measured by bio-layer interferometry (BLI). Shown in (f) are the 6 RBM-targeting mAbs with reduced binding to N501Y RBD and 2 representative mAbs (RBM-targeting S2E12 and non-RBM-targeting S2X35). Area under the curve (AUC) (g) and AUC fold change (h) of 51 mAbs tested against WT and N501Y RBD. mAbs with a >1.3 AUC fold change shown in blue.

Figure 3

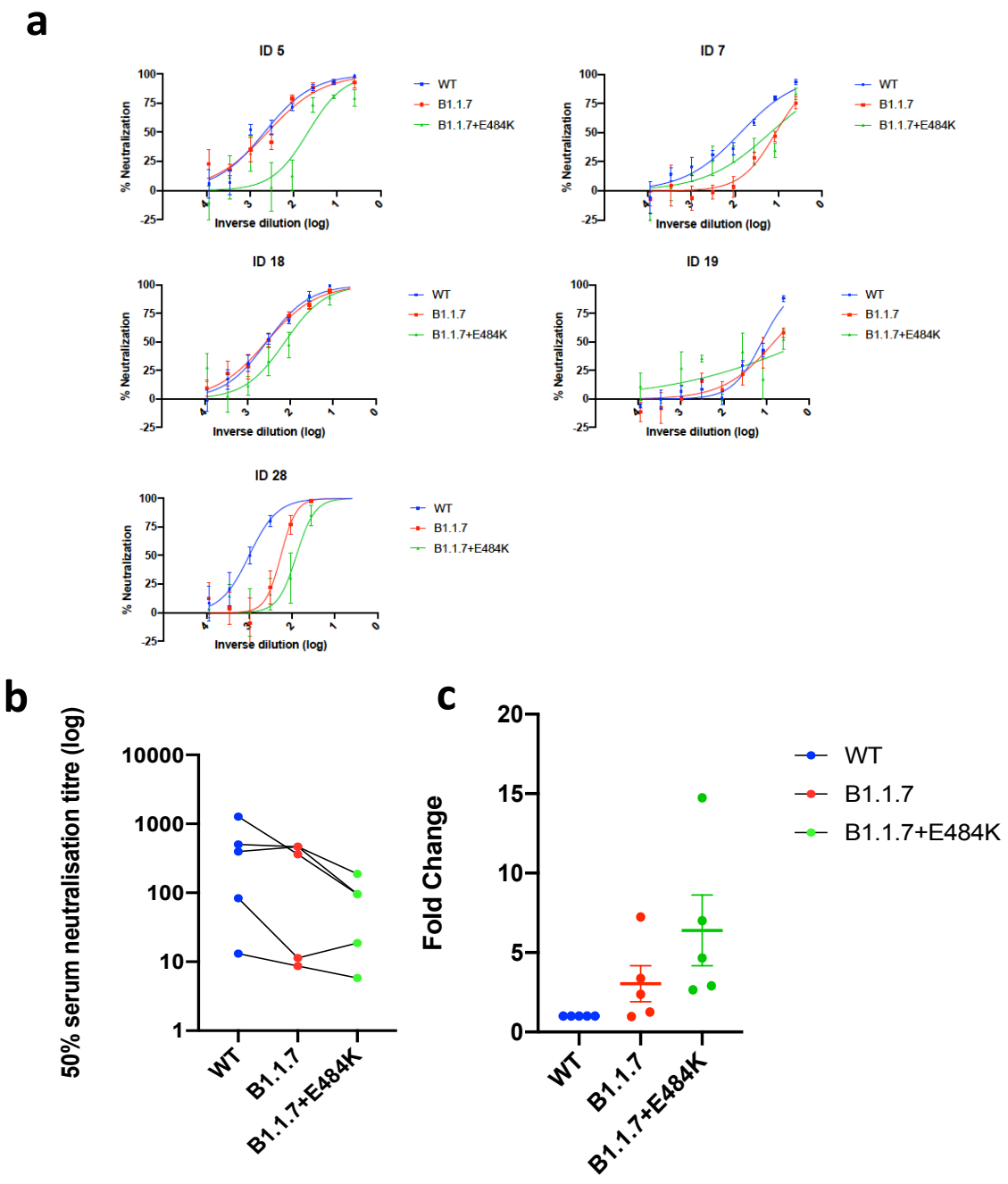

Figure 4. Neutralisation potency of vaccine sera against pseudovirus virus bearing Spike mutations in the B1.1.7 lineage with and without E484K in the receptor binding domain (all In Spike D614G background). **a,** Neutralisation curves for five vaccinated individuals. **b.** Indicated is 50% neutralisation titre for each virus and in **c.** data are expressed as fold change relative to WT. Data points represent means of two independent experiments.

Extended Data Figure 1

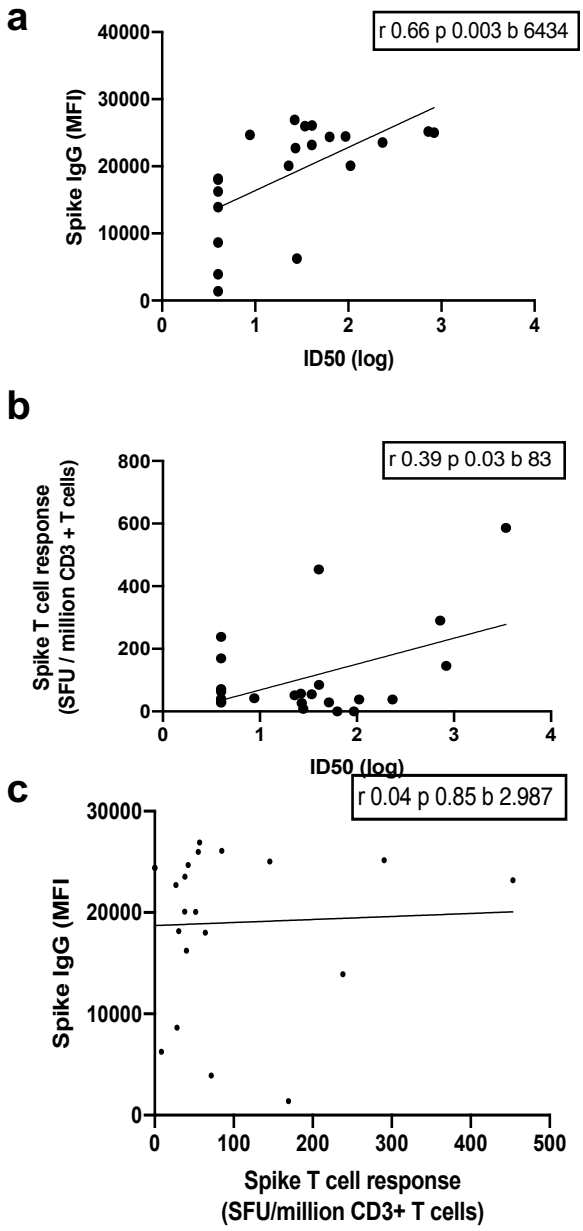

Extended Data Figure 1: Immune responses three weeks after first dose of Pfizer SARS-CoV-2 vaccine BNT162b2 a, Relationship between serum IgG responses as measured by flow cytometry and serum neutralisation ID50. **b,** Relationship between serum neutralisation ID50 and T cell responses against SARS-CoV-2 by IFN gamma ELISPOT. SFU: spot forming units. **c**, Relationship between serum IgG responses and T cell responses.

Extended Data Fig. 2

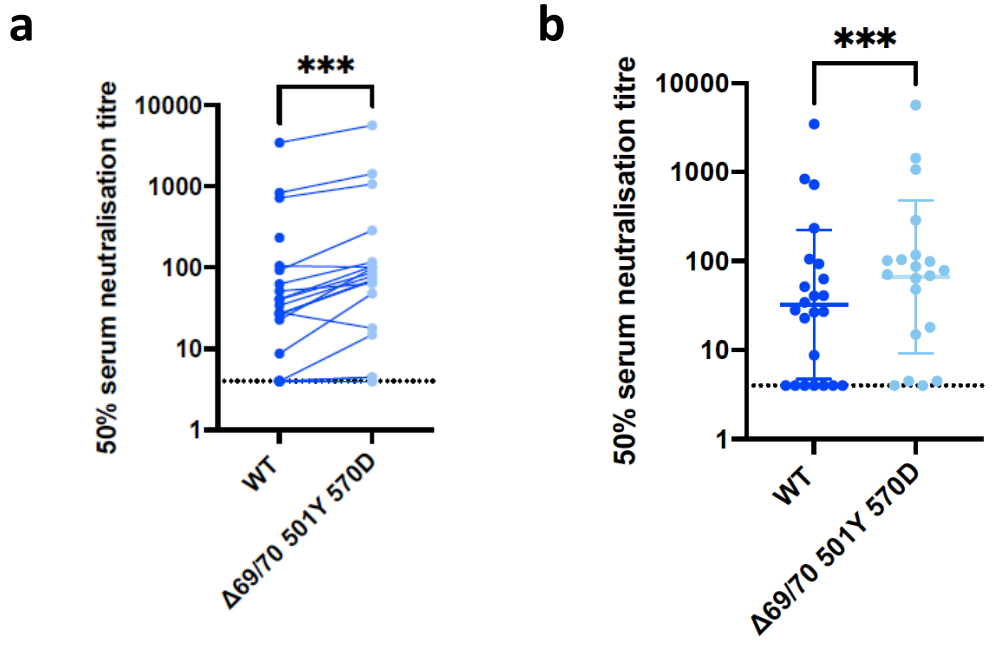

Extended data Fig 2. Neutralisation by vaccine sera against wild type and mutant SARS-CoV-2 pseudotyped viruses: (**a-b**) WT and Spike mutant with N501Y, A570D, **Δ**H69/V70. Data are representative of 2 independent experiments.

Extended Data Fig. 3

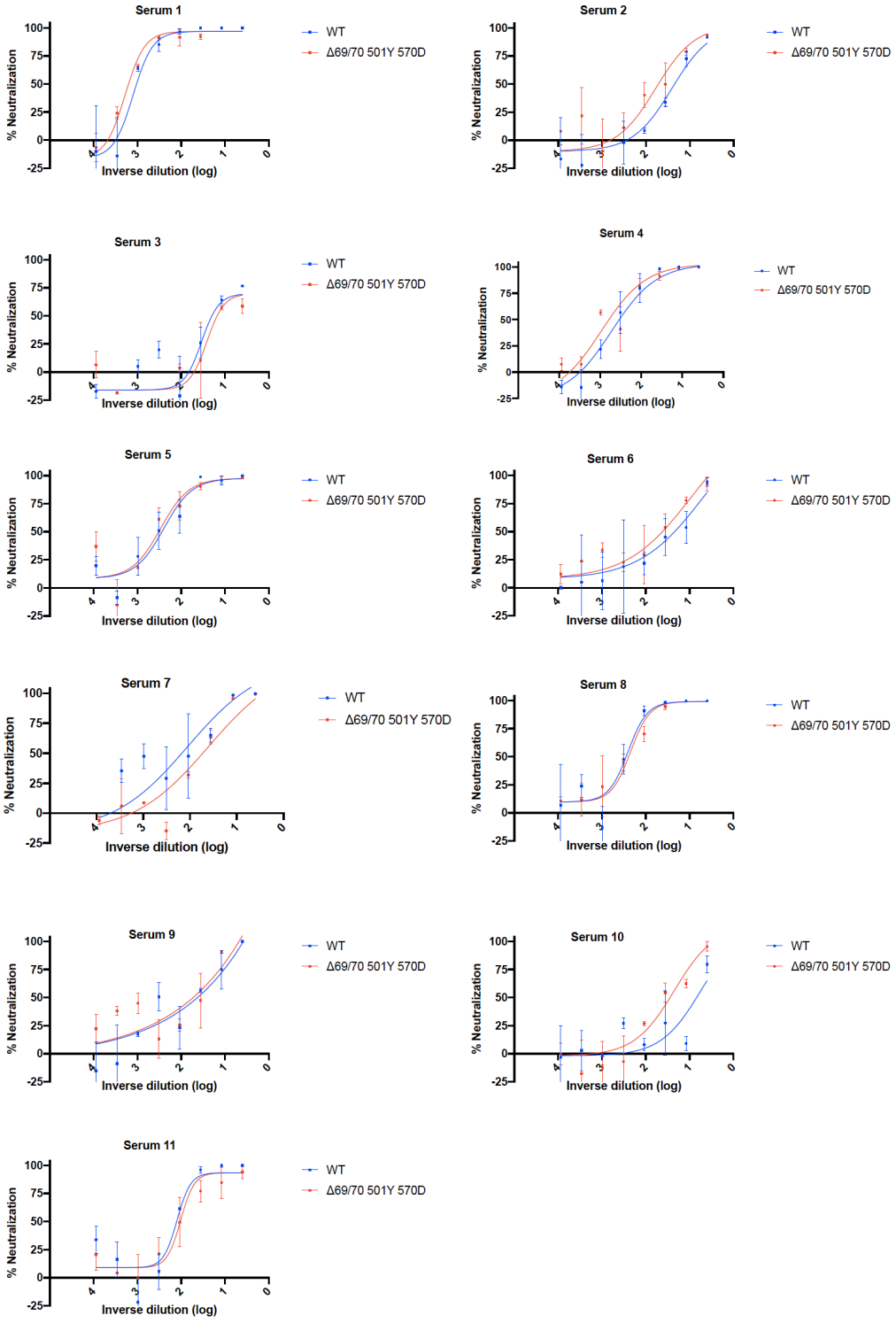

Extended Data Fig. 3. Neutralisation potency of convalescent sera against pseudovirus virus bearing three Spike mutations (N501Y, A570D, ΔH69/V70) present in B.1.1.7 versus wild type (all In Spike D614G background). Indicated is serum $\log_{10}$ inverse dilution against % neutralisation. Where a curve is shifted to the right this indicates the virus is less sensitive to the neutralising antibodies in the serum. Data points represent means of technical replicates and error bars represent standard error of the mean.

Extended Data Fig. 4

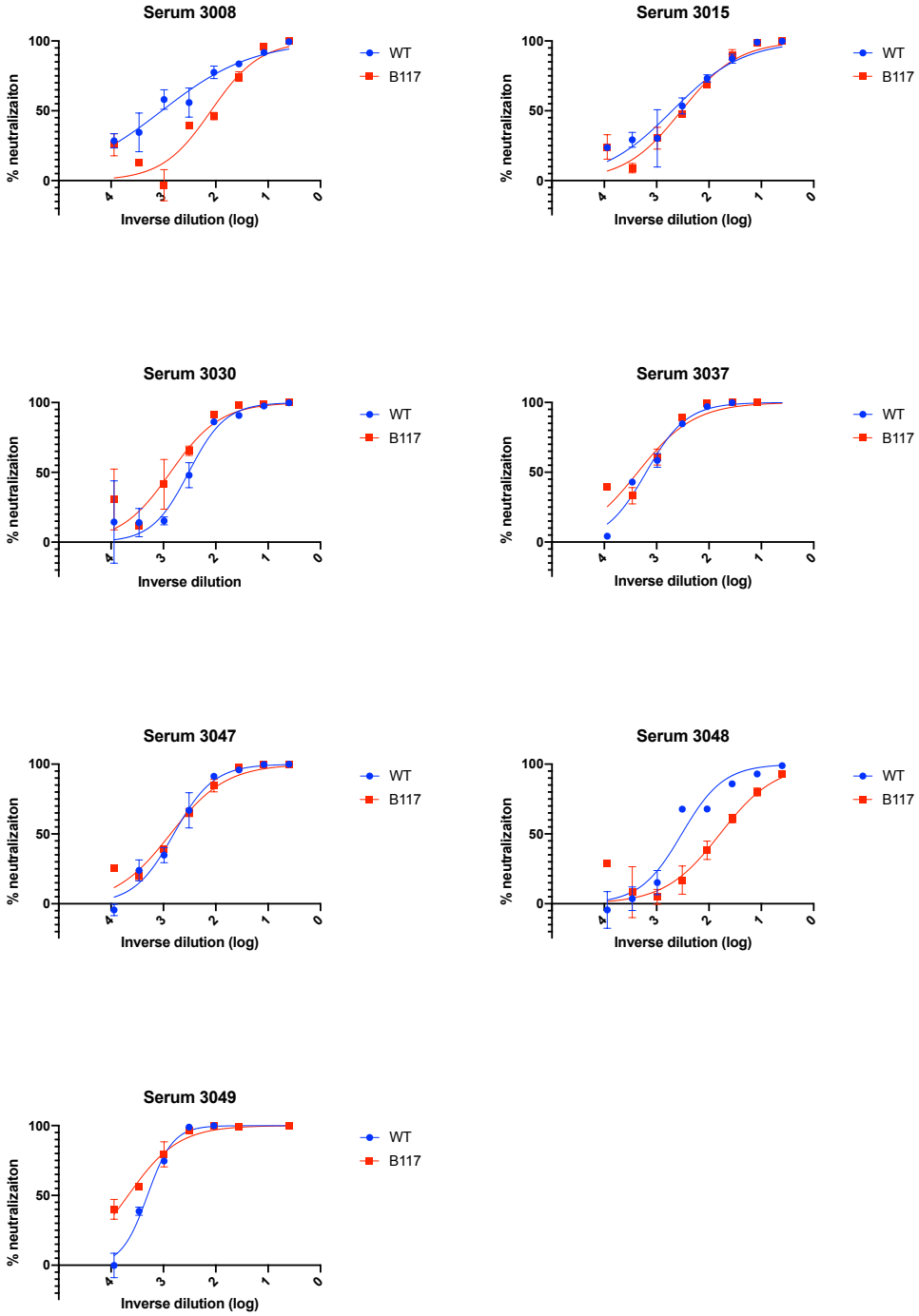

Extended Data Fig. 4. Neutralisation potency of convalescent sera against wild type and B.1.1.7 Spike mutant SARS-CoV-2 pseudoviruses. Indicated is serum $\log_{10}$ inverse dilution against % neutralisation. Where a curve is shifted to the right this indicates the virus is less sensitive to the neutralising antibodies in the serum. Data points represent means of technical replicates and error bars represent standard error of the mean.

Extended Data Fig. 5

Extended Data Fig. 5. Neutralisation of WT and B.1.1.7 SARS-CoV-2 of a panel of 58 mAbs. **a-c,** Neutralisation of WT (black) and B.1.1.7 (orange) SARS-CoV-2-MLV by 9 NTD-targeting (a), 27 RBM-targeting (b) and 22 non-RBM-targeting (c) mAbs**.**

Extended Data Fig. 6

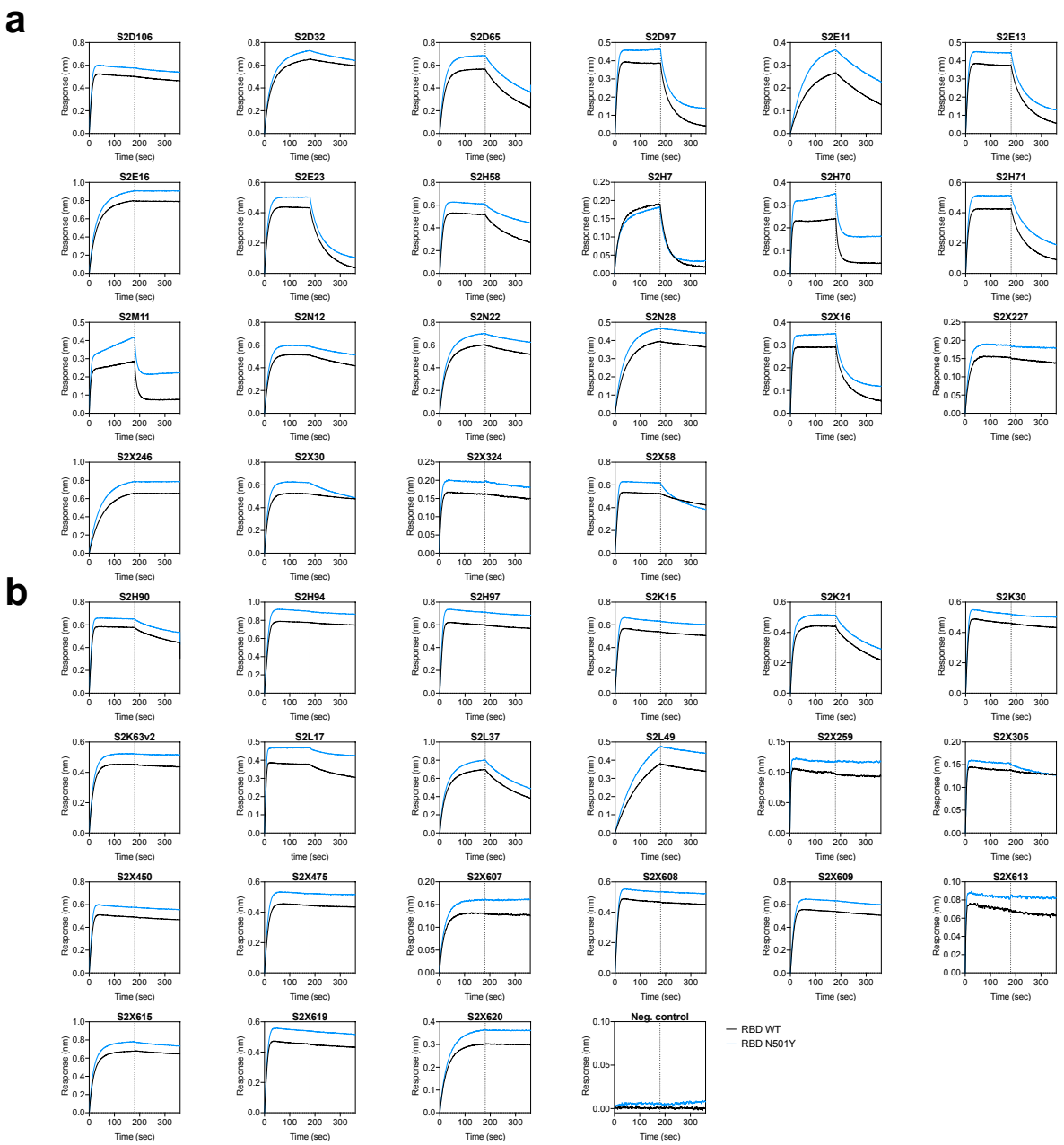

Extended Data Fig. 6. Kinetics of binding to WT and N501Y SARS-CoV-2 RBD of 43 RBD-specific mAbs. a-b, Binding to WT (black) and N501Y (blue) RBD by 22 RBM-targeting (a) and 21 non-RBM-targeting (b) mAbs. An antibody of irrelevant specificity was included as negative control.

Extended Data Fig. 7

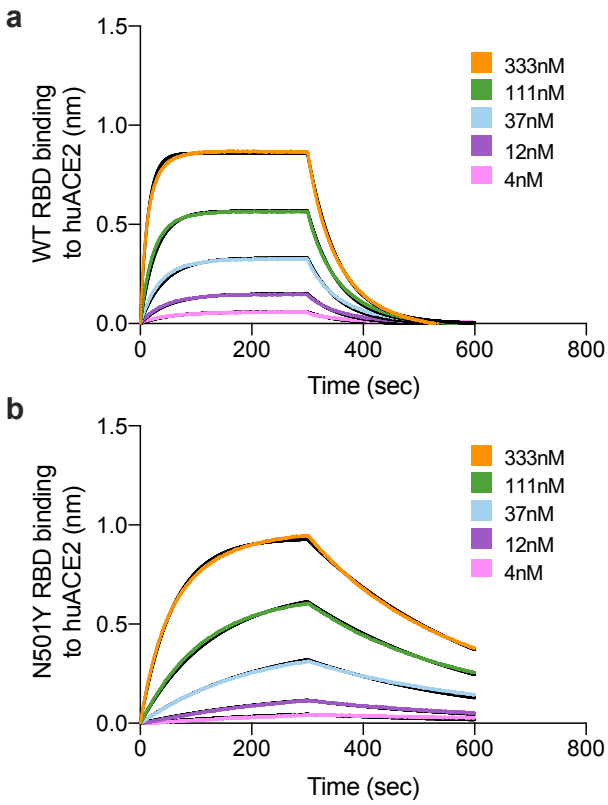

Extended Data Fig. 7. Binding of human ACE2 to SARS-CoV-2 B.1.1.7 and WT RBDs. a-b. BLI binding analysis of the human ACE2 ectodomain (residues 1-615) to immobilized SARS-CoV-2 WT RBD (a) and B.1.1.7 RBD (b) or. Black lines correspond to a global fit of the data using a 1:1 binding model.